



Numerical study of collisional particle dynamics in cluster-induced turbulence

Jesse Capecelatro^{1,†}, Olivier Desjardins¹ and Rodney O. Fox^{2,3}

¹Sibley School of Mechanical and Aerospace Engineering, Cornell University, Ithaca, NY 14853-7501, USA

²Department of Chemical and Biological Engineering, 2114 Sweeney Hall, Iowa State University, Ames, IA 50011-2230, USA

³EM2C-UPR CNRS 288, Ecole Centrale Paris, Grande voie des Vignes, 92295 Chatenay Malabry, France

(Received 19 February 2014; revised 1 April 2014; accepted 4 April 2014)

We present a computational study of cluster-induced turbulence (CIT), where the production of fluid-phase kinetic energy results entirely from momentum coupling with finite-size inertial particles. A separation of length scales must be established when evaluating the particle dynamics in order to distinguish between the continuous mesoscopic velocity field and the uncorrelated particle motion. To accomplish this, an adaptive spatial filter is employed on the Lagrangian data with an averaging volume that varies with the local particle-phase volume fraction. This filtering approach ensures sufficient particle sample sizes in order to obtain meaningful statistics while remaining small enough to avoid capturing variations in the mesoscopic particle field. Two-point spatial correlations are computed to assess the validity of the filter in extracting meaningful statistics. The method is used to investigate, for the first time, the properties of a statistically stationary gravity-driven particle-laden flow, where particle–particle and fluid–particle interactions control the multiphase dynamics. Results from fully developed CIT show a strong correlation between the local volume fraction and the granular temperature, with maximum values located at the upstream boundary of clusters (i.e. where maximum compressibility of the particle velocity field exists), while negligible particle agitation is observed within clusters.

Key words: homogeneous turbulence, multiphase and particle-laden flows, particle/fluid flow

1. Introduction

The non-trivial interphase coupling encountered in disperse two-phase flows can often lead to a high degree of segregation from an initially homogeneous distribution of particles. For example, when subjected to turbulence, the disperse phase may be

† Email address for correspondence: jsc359@cornell.edu

ejected from regions of high vorticity and accumulate in regions of high strain (e.g. Balachandar & Eaton 2010, and references therein), and under the influence of gravity, momentum coupling between the phases may lead to the spontaneous generation of dense clusters (e.g. Agrawal *et al.* 2001; Capecelatro, Pepiot & Desjardins 2014). In fluidized bed reactors, clusters have been observed to reduce mixing and interaction of particles with the transport gas (Shaffer *et al.* 2013), and may therefore inhibit reaction rates and heat transfer, potentially lowering operating efficiencies significantly. Meanwhile, a fundamental understanding of cluster characteristics and their effect on the carrier phase remains elusive.

In the context of high-inertia particles with response times that are long compared with the characteristic time scale of the turbulence, individual particle trajectories will retain information from previous collisions and interactions with distant turbulent eddies, causing them to deviate from fluid pathlines (Maxey 1987). The velocities of neighbouring particles may therefore be uncorrelated, while ensembles of particles collectively respond to large-scale motions of the flow. Dasgupta, Jackson & Sundaresan (1994) first suggested that the fluctuating particle motion can be partitioned into a smooth (continuous) field and a random component at the particle scale referred to as the granular temperature. Later, Février, Simonin & Squires (2005) provided an exact definition and a computational methodology for partitioning of the correlated and uncorrelated contributions to the total particle-phase kinetic energy. In a recent study, Fox (2014) provided a rigorous derivation of a Reynolds-average turbulence model for collisional fluid–particle flows, demonstrating that the transport equations must contain separate models for these two contributions. It was shown that new turbulence production terms arise due to correlations between the particle-phase volume fraction and fluid-phase velocity fluctuations. At sufficient mass loadings, the fluid–particle correlations become significant in systems with large variations in particle concentration. In the absence of mean shear, the production of fluid-phase kinetic energy results entirely from momentum coupling between the phases, referred to as cluster-induced turbulence (CIT).

Various mechanisms responsible for the spatial segregation of particles have been studied extensively in the last two decades. In purely granular systems, clustering is enhanced via inelastic dissipation (Hopkins & Louge 1991; Goldhirsch & Zanetti 1993) and attenuated via friction (Royer *et al.* 2009; Mitrano *et al.* 2013) during interparticle contact. In the presence of a carrier phase, viscous damping by the fluid results in clustering of non-dissipative particles (Wylie & Koch 2000). In a recent study, Yin *et al.* (2013) compared the relative contributions of these instabilities in dissipative gas–solid systems. One of the most widely investigated mechanisms is preferential concentration of particles by coherent vortical structures, first realized numerically by Eaton & Fessler (1994). Preferential concentration occurs in the absence of a mean velocity difference between the phases and is most obvious for dilute flows with low mass loading. When fluid–particle systems are subjected to a mean body force (e.g. gravity), the relative motion between the phases leads to additional sources of instability as a result of interphase coupling (Glasser, Sundaresan & Kevrekidis 1998), giving rise to CIT. While progress in understanding dissipative instabilities and preferential concentration continues to be made, much less is known about CIT. The production of large-scale fluid turbulence from particle clusters was first observed in simulations of a two-dimensional vertical channel by Tsuji, Tanaka & Yonemura (1994). In our previous work (Capecelatro *et al.* 2014), it was demonstrated that the cluster size distribution in wall-bounded flows is constrained by the flow geometry. It was also shown that the multiphase dynamics in two dimensions differs

significantly from three-dimensional flow. Three-dimensional homogeneous flows therefore represent the simplest configuration to study fully developed CIT.

With the availability of increasing computational resources, detailed simulations are now able to capture such phenomena at moderate Reynolds numbers and particle concentrations. In order to develop an improved understanding of the fundamental nature of such flows, and to exploit these simulations to aid in model development, it is necessary to extract local instantaneous information in a consistent and accurate manner. The objective of the present work is to evaluate the spatial characteristics of finite-size inertial particles in a fully coupled turbulent flow, where interparticle collisions and momentum coupling between the phases control the flow dynamics. Fully developed gravity-driven CIT is simulated via an Eulerian–Lagrangian framework, where the unsteady fluid motion is sufficiently captured by the mesh and the two phases are coupled through the resolved contributions of the fluid stresses and a drag term. An adaptive spatial filter is introduced which accurately decouples the instantaneous particle-phase turbulent kinetic energy from the granular temperature, providing, for the first time, access to the local instantaneous spatial distribution of these separate contributions in an Eulerian framework.

2. Volume-filtered Euler–Lagrange formalism

In order to resolve the relevant length scales associated with fully developed CIT while remaining computationally tractable, we employ a mesoscopic formulation based on volume filtering to describe the fluid–particle system. The mesoscale description of fluid–particle flows refers to a set of equations that explicitly captures the physics associated with length scales larger than the individual particles and models the processes at the particle scale. Unlike in particle-resolved direct numerical simulation (DNS), where the boundary layers are solved around individual particles (see e.g. Tenneti & Subramaniam 2014), in mesoscopic formulations the two phases are coupled via momentum exchange terms (e.g. a drag model) (Fox 2012). This level of modelling is similar to large-eddy simulation (LES) of single-phase turbulence, where the large-scale unsteady motions are represented explicitly and the effects of the smaller-scale motions are modelled. However, unlike in LES, these small-scale motions are not universal, and fluid-phase velocity fluctuations may arise from granular agitation at the particle scale, due, for example, to wakes and interparticle collisions. Given an accurate and consistent set of models for the particle-scale dynamics, and assuming that mesoscale structures in the flow (e.g. clusters) are sufficiently resolved and are responsible for generating the majority of fluid-phase velocity fluctuations, this framework has been shown to accurately reproduce the relevant physics in two-way coupled fluid–particle flows (Capecehatro & Desjardins 2013; Capecehatro *et al.* 2014).

2.1. Description of the system

To isolate the effect of turbulence generated by interphase coupling, we consider a flow initially at rest laden with a random distribution of finite-size particles of diameter d_p subject to gravity. The physical parameters are chosen to correspond to typical gas–solid flows encountered in engineering and environmental applications. The dimensionless two-phase parameters that characterize the flow include the particle to fluid density ratio $\rho_p/\rho_f = 1000$, the average particle-phase volume fraction $\langle\alpha_p\rangle = 0.01$ and the Reynolds number $Re = \tau_p g d_p / \nu_f = 1$, where $\tau_p = \rho_p d_p^2 / (18 \rho_f \nu_f)$ is the particle response time, ν_f is the fluid-phase kinematic viscosity and g is the

magnitude of the gravity vector \mathbf{g} . Combination of these non-dimensional numbers yields the mass loading $\phi = \rho_p \langle \alpha_p \rangle / (\rho_f \langle \alpha_f \rangle) = 10$, where $\langle \alpha_f \rangle = 1 - \langle \alpha_p \rangle$ is the average fluid-phase volume fraction. To obtain an *a priori* measure of the mesoscale features that arise due to the coupling between the phases, previous studies have introduced a characteristic length scale $\mathcal{L} = \tau_p^2 g$ (see e.g. Agrawal *et al.* 2001; Igci *et al.* 2008; Ozel, Fede & Simonin 2013). This length scale is used in this work to ensure an appropriate domain size such that the effect of the periodic boundary conditions is minimized. The simulation is solved on a triply periodic domain of dimensions $64\mathcal{L} \times 16\mathcal{L} \times 16\mathcal{L}$, with a mesh size of $2048 \times 512 \times 512$, corresponding to a uniform grid spacing of $\Delta x = 1.75d_p$, with 55×10^6 particles.

2.2. Gas–solid description

The flow of solid spherical particles suspended in an incompressible carrier fluid is solved in an Eulerian–Lagrangian framework, where the displacement of an individual particle i is calculated using Newton’s second law of motion,

$$\frac{d\mathbf{u}_p^{(i)}}{dt} = \mathcal{A}^{(i)} + \mathbf{F}_c^{(i)} + \mathbf{g}, \quad (2.1)$$

where $\mathbf{u}_p = (u_p, v_p, w_p)$ is the instantaneous particle velocity vector, \mathcal{A} is the interphase exchange term and \mathbf{F}_c is the collision force modelled using a modified soft-sphere approach originally proposed by Cundall & Strack (1979). In this work, we consider inelastic collisions with a coefficient of restitution $e = 0.9$. The interphase exchange term is given by

$$\mathcal{A}^{(i)} = \frac{1}{\tau_p} (\mathbf{u}_f[\mathbf{x}_p^{(i)}] - \mathbf{u}_p^{(i)}) - \frac{1}{\rho_p} \nabla p_f^*[\mathbf{x}_p^{(i)}] + \frac{1}{\rho_p} \nabla \cdot \sigma_f[\mathbf{x}_p^{(i)}], \quad (2.2)$$

where the fluid-phase velocity vector $\mathbf{u}_f = (u_f, v_f, w_f)$, modified pressure gradient ∇p_f^* and divergence of the viscous stress tensor $\nabla \cdot \sigma_f$ are taken at $\mathbf{x}_p^{(i)}$, the centre position of particle i . The term ∇p_f^* is a body force that contains the hydrodynamic pressure p_f and is adjusted dynamically in order to maintain statistically stationary CIT. In real systems with moderate Reynolds numbers and particle volume fractions, the particles will experience drag with a nonlinear dependence on these terms (e.g. Tenneti, Garg & Subramaniam 2011), but for consistency with Fox (2014), the higher-order terms are neglected here. To account for the presence of the particle phase in the fluid without requiring resolution of the boundary layers around individual particles, a volume filter is applied to the constant-density Navier–Stokes equations (Anderson & Jackson 1967), thereby replacing the point variables (fluid velocity, pressure, etc.) by smoother locally filtered fields. The resulting fluid-phase equations are given by

$$\frac{\partial \alpha_f}{\partial t} + \nabla \cdot (\alpha_f \mathbf{u}_f) = 0 \quad (2.3)$$

and

$$\frac{\partial \alpha_f \mathbf{u}_f}{\partial t} + \nabla \cdot (\alpha_f \mathbf{u}_f \otimes \mathbf{u}_f) = -\frac{1}{\rho_f} \nabla p_f^* + \frac{1}{\rho_f} \nabla \cdot \sigma_f - \frac{\rho_p}{\rho_f} \alpha_p \tilde{\mathcal{A}} + \alpha_f \mathbf{g}. \quad (2.4)$$

The relationship between the interphase exchange term seen by the fluid, $\tilde{\mathcal{A}}$, and that seen by an individual particle i , $\mathcal{A}^{(i)}$, will be made explicit in § 2.3. Further details on the numerical implementation can be found in Capecelatro & Desjardins (2013).

2.3. Two-way coupling

To interpolate the fluid variables to the particle location, a second-order trilinear interpolation scheme is used. To extrapolate the particle data back to the Eulerian mesh, we apply the volume filtering approach used in deriving the fluid-phase equations of motion (2.3) and (2.4). We begin by defining a filtering kernel G with a characteristic length δ_f , such that $G(r) > 0$ decreases monotonically with increasing r , and is normalized such that it integrates to unity. Given a quantity $A^{(i)}(t)$ located at the centre of particle i at time t , and assuming that G does not vary significantly over the volume of the particle (i.e. $\delta_f \gg d_p$), its Eulerian projection is given by

$$\alpha_p \tilde{A}(\mathbf{x}, t) \approx \sum_{i=1}^{N_p} A^{(i)}(t) G(|\mathbf{x} - \mathbf{x}_p^{(i)}|) V_p, \quad (2.5)$$

where N_p is the total number of particles in a single realization of the flow and $V_p = \pi d_p^3/6$ is the particle volume. This expression replaces the discontinuous Lagrangian data with an Eulerian field that is a smooth function of the spatial coordinate \mathbf{x} . Using (2.5) with $A^{(i)} = 1$, we obtain the particle volume fraction α_p , and $A^{(i)} = \mathcal{A}^{(i)}$ gives the momentum exchange term $\tilde{\mathcal{A}}$ seen by the fluid in (2.4).

It should be noted that (2.5) will only yield useful information if the spatial variations in the particle field can be decomposed into contributions on a scale comparable with the particle spacing and a much larger scale corresponding to mesoscopic features in the flow (e.g. clusters), provided that the filter size δ_f is within these scales. For ratios of $\Delta x/d_p \approx 1$, a brute-force implementation of (2.5) would require looping through a large number of cells for each particle, making this operation prohibitively expensive. Therefore, the filtering procedure is solved in two steps (Capecehatro & Desjardins 2013). First, the particle data are transferred to the nearest neighbouring cells via trilinear extrapolation. The data are then diffused such that the final width of the filtering kernel is independent of the mesh size. In this work, G is taken to be Gaussian with a characteristic length scale $\delta_f = 8d_p$, defined as the full width at half the height of the kernel. This value of δ_f will be justified in §3.3. To keep the cost low and ensure unconditional stability, the diffusion process is solved in a single implicit step by utilizing the approximate factorization scheme of Briley & McDonald (1977).

3. Results and discussion

3.1. Degree of particle segregation

The simulation is run until the initial transient is complete and the flow reaches a statistically stationary state. Throughout this study, the subscript ‘1’ is used to denote components in the streamwise (gravity-aligned) direction, and the spanwise directions are denoted by subscripts ‘2’ and ‘3’. As depicted in figure 1(a), the resulting particle field is highly unsteady with strong segregation in volume fraction. Figure 1(b) suggests that the fluid phase is entrained by the clusters, leading to strong vertical velocities in dilute regions of the flow. This behaviour is evident in figure 2(a), where the vertical slip velocity between the phases is observed to decrease with increasing volume fraction. The degree of particle segregation can be quantified by the probability density function (p.d.f.) of the particle volume fraction (Pozorski & Apte 2009). For a homogeneous distribution of particles, the p.d.f. is given by the discrete Poisson distribution (Squires & Eaton 1991). As seen in

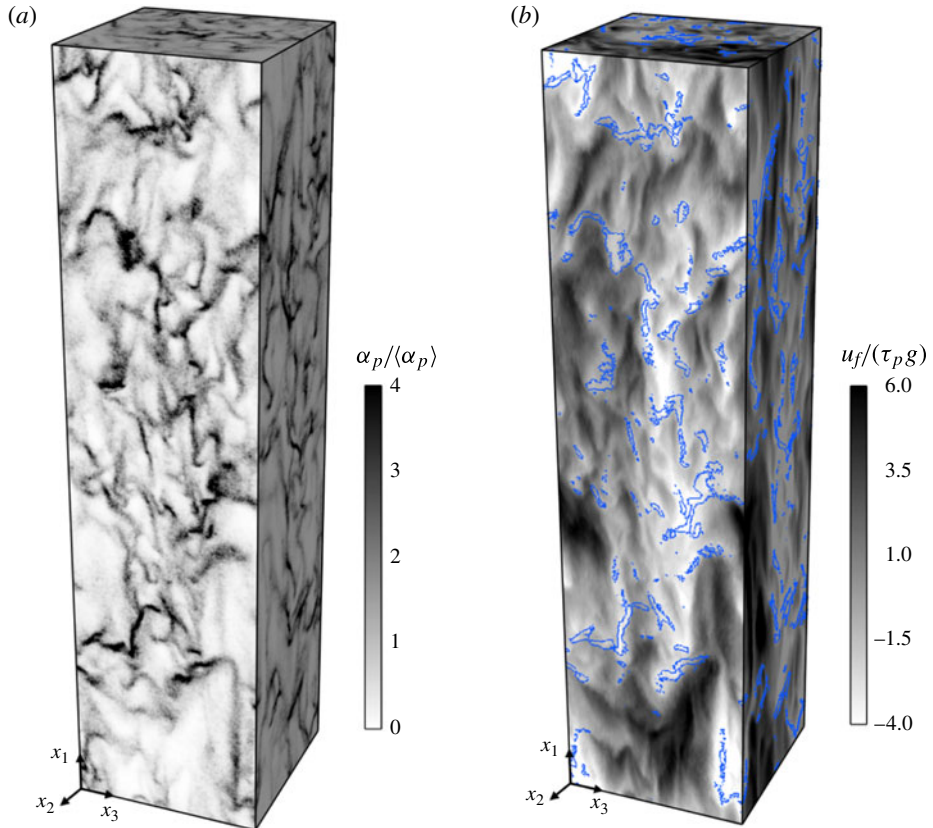


FIGURE 1. The instantaneous field of fully developed CIT showing (a) the particle-phase volume fraction and (b) the vertical component of the fluid velocity with isocontours of $\alpha_p = 3\langle\alpha_p\rangle$ shown in blue.

figure 2(b), the instantaneous particle field displays a higher frequency of regions containing more particles, as well as regions devoid of particles, in comparison with the Poisson distribution, indicative of a highly clustered field. Moreover, using the mean and variance particle volume fraction extracted from the simulation, the form of the p.d.f. is seen to closely resemble a log-normal distribution, indicating a potential opportunity for future modelling efforts.

3.2. *Spatial decomposition of the particle velocity field*

The averaging operator $\langle(\cdot)\rangle$ is used throughout to denote a particle average when applied to a Lagrangian quantity and a volume average when applied to an Eulerian quantity. Due to the statistical stationarity of the flow, $\langle(\cdot)\rangle$ is neither a function of the spatial coordinate \mathbf{x} nor of time t at steady state. For a single realization of the flow, the total particle-phase fluctuating energy is given by

$$\kappa_p = \frac{1}{2} \langle \mathbf{u}'_p \cdot \mathbf{u}'_p \rangle, \quad (3.1)$$

where $\mathbf{u}'_p = \mathbf{u}_p - \langle \mathbf{u}_p \rangle$ is the total fluctuation in particle velocity with the property $\langle \mathbf{u}'_p \rangle = 0$. In order to decompose κ_p into its spatially correlated contribution and fluctuations

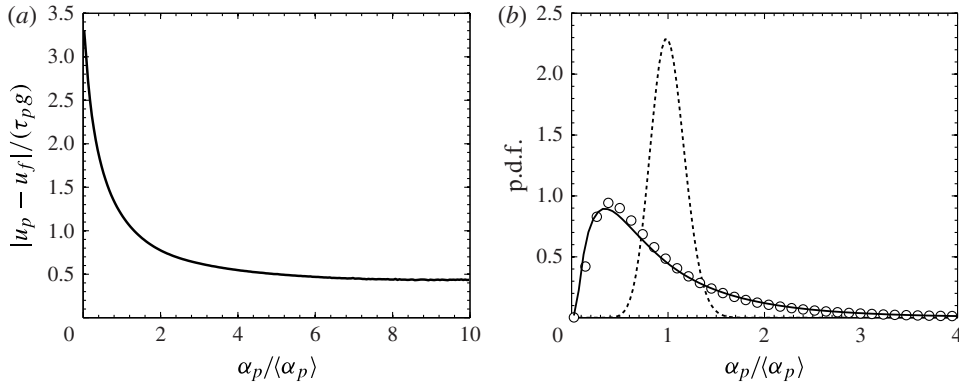


FIGURE 2. Results from a single realization of fully developed CIT: (a) the normalized slip velocity conditioned on α_p ; (b) the p.d.f. of α_p (—), the corresponding log-normal distribution (○) and the Poisson distribution (---).

at the particle scale, the volume filtering procedure discussed in § 2.3 is employed. By applying $A^{(i)} = \mathbf{u}_p^{(i)}$ in (2.5), we obtain the local mean particle velocity $\tilde{\mathbf{u}}_p$ in an Eulerian frame of reference. Analogous to Favre averaging in variable-density flows, the phase average (PA) denoted by $\langle (\cdot) \rangle_p = \langle \alpha_p (\cdot) \rangle / \langle \alpha_p \rangle$ is useful in multiphase modelling. Note that PA Eulerian terms are identical to particle-average Lagrangian terms, e.g. $\langle \tilde{\mathbf{u}}_p \rangle_p = \langle \mathbf{u}_p \rangle$. Fluctuations about the PA velocity are expressed as $\tilde{\mathbf{u}}_p''(\mathbf{x}, t) = \tilde{\mathbf{u}}_p(\mathbf{x}, t) - \langle \tilde{\mathbf{u}}_p \rangle_p$, with $\langle \tilde{\mathbf{u}}_p'' \rangle_p = 0$. It is important to note that $\mathbf{u}'_p \neq \tilde{\mathbf{u}}_p''$, and therefore $\langle \tilde{\mathbf{u}}_p'' \rangle_p \neq 0$ in general. Using this definition, the PA particle turbulent kinetic energy is defined as

$$k_p = \frac{1}{2} \langle \tilde{\mathbf{u}}_p'' \cdot \tilde{\mathbf{u}}_p'' \rangle_p. \quad (3.2)$$

A quantitative measure of the local uncorrelated particle agitation is given by the granular temperature Θ , which is defined using the residual component of the instantaneous particle velocity,

$$\Theta(\mathbf{x}, t) = \frac{1}{3} \delta \mathbf{u}_p(t) \cdot \widetilde{\delta \mathbf{u}_p(t)}, \quad (3.3)$$

where $\delta \mathbf{u}_p(t) = \mathbf{u}_p(t) - \tilde{\mathbf{u}}_p[\mathbf{x}_p(t), t]$. With these definitions, the total particle-phase fluctuating energy κ_p corresponds to the sum of the PA turbulent kinetic energy k_p and the PA granular temperature $\langle \Theta \rangle_p$. The distinction between k_p and $\langle \Theta \rangle_p$ is crucial in turbulence modelling. For instance, in the context of moderately dense particulate flows, $\langle \Theta \rangle_p$ is needed to evaluate the particle-phase viscosity and pressure, which arise due to collisions. Thus, failure to separate these two contributions will lead to a gross overprediction of the collision rate (Fox 2014). Moreover, previous works (Hrenya & Sinclair 1997; Février *et al.* 2005) have shown that the dissipation of k_p enters as a source term for $\langle \Theta \rangle_p$. This is analogous to single-phase flow where dissipation of turbulent kinetic energy leads to viscous heating.

3.3. The filtering procedure for the extraction of particle statistics

Evaluation of the particle-phase statistics, in particular k_p and $\langle \Theta \rangle_p$, requires the introduction of a separation of length scales into the averaging procedure. To

accomplish this, we employ an averaging volume that adapts to the local particle field, allowing for a sufficient number of particles to be sampled in dilute regions of the flow, while remaining optimally compact in dense clusters. Given an ensemble of identical (i.e. monodisperse) particles, and assuming that there are no sharp gradients in the volume fraction, an averaging volume will sample \mathcal{N}_p particles with a filter size

$$\delta_f(\alpha_p) = \left(\frac{\mathcal{N}_p d_p^3}{\alpha_p} \right)^{1/3}. \quad (3.4)$$

Since δ_f is a function of α_p , which itself is a filtered quantity and is thus a function of δ_f , (3.4) cannot be solved directly. Instead, α_p is initially computed with a constant filter size $\delta_{f,0}$, which is then applied to (3.4). The resulting volume fraction field can then be used to recompute (3.4) in an iterative process. It was found that α_p converges rapidly to a reference solution regardless of the choice of $\delta_{f,0}$ or \mathcal{N}_p . Negligible error was observed after a single iteration, with values of $\delta_{f,0} = 8d_p$ and $\mathcal{N}_p = 10$ yielding the best results.

While the accuracy of the instantaneous multiphase statistics is dependent upon the sample size used when averaging, two-point Lagrangian statistics account for the spatial distribution of particles as a continuous function of particle-pair separation and therefore do not require a specific averaging volume. Thus, they can be used to assess the accuracy of the filtering procedure in extracting Lagrangian data. An important statistical measure of the spatial distribution of particles is the radial distribution function (r.d.f.), defined as the number of particle pairs found at a given separation normalized by the expected number of pairs found in a homogeneous distribution (McQuarrie 1976). It can be expressed as

$$g_0(\mathbf{r}\mathbf{e}_i) = \frac{\left\langle \sum_{m=1}^{N_p} \sum_{n \neq m}^{N_p} \delta(\mathbf{x} - \mathbf{x}_p^{(m)}) \delta(\mathbf{x} + \mathbf{r}\mathbf{e}_i - \mathbf{x}_p^{(n)}) \right\rangle}{\left\langle \sum_{m=1}^{N_p} \delta(\mathbf{x} - \mathbf{x}_p^{(m)}) \right\rangle \left\langle \sum_{m=1}^{N_p} \delta(\mathbf{x} + \mathbf{r}\mathbf{e}_i - \mathbf{x}_p^{(m)}) \right\rangle}, \quad (3.5)$$

where δ is the Dirac delta function, $r \geq d_p$ is the separation between two particles $n \neq m$ and \mathbf{e}_i is the unit normal vector in the i direction. With this definition, $g_0 = 1$ represents a homogeneous distribution of particles and $g_0 > 1$ implies clustering. Similarly, we define the trace of the two-point velocity correlation as

$$R(\mathbf{r}\mathbf{e}_i) = \frac{1}{2} \frac{\left\langle \sum_{m=1}^{N_p} \sum_{n \neq m}^{N_p} \delta(\mathbf{x} - \mathbf{x}_p^{(m)}) \delta(\mathbf{x} + \mathbf{r}\mathbf{e}_i - \mathbf{x}_p^{(n)}) \mathbf{u}_p^{(m)} \cdot \mathbf{u}_p^{(n)} \right\rangle}{\left\langle \sum_{m=1}^{N_p} \sum_{n \neq m}^{N_p} \delta(\mathbf{x} - \mathbf{x}_p^{(m)}) \delta(\mathbf{x} + \mathbf{r}\mathbf{e}_i - \mathbf{x}_p^{(n)}) \right\rangle}. \quad (3.6)$$

Due to the homogeneity of the flow, (3.5) and (3.6) are functions of the pair separation only, but in the presence of gravity the statistics may exhibit strong anisotropy and therefore depend strongly on the directionality of $\mathbf{r}\mathbf{e}_i$.

Starting from the one-particle p.d.f., Février *et al.* (2005) showed that for dilute (non-collisional) suspensions of inertial particles in isotropic turbulence, two-point

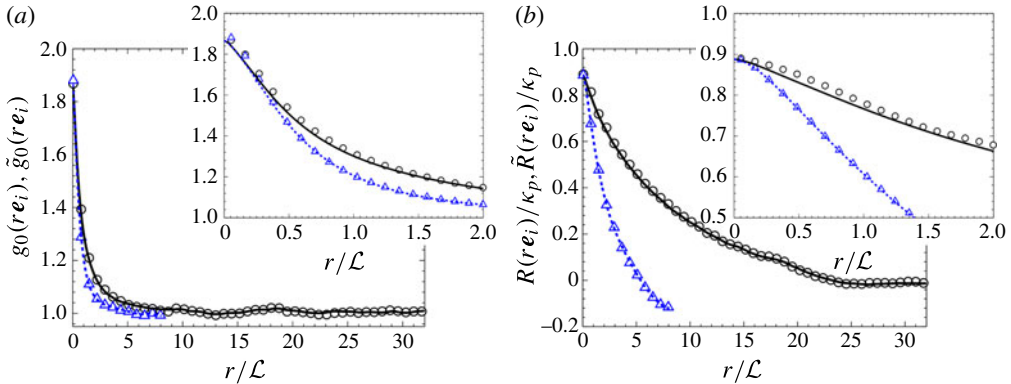


FIGURE 3. Comparison of Lagrangian and Eulerian two-point statistics showing (a) the r.d.f. and (b) normalized two-point velocity correlations. The lines correspond to Eulerian statistics obtained with the adaptive filter (3.4) with $\delta_{f,0} = 8d_p$ and $\mathcal{N}_p = 10$, and the symbols correspond to two-point Lagrangian statistics. The black lines and circles correspond to a pair separation computed in the streamwise direction ($\mathbf{r}e_1$), and the blue dashed lines and triangles correspond to a pair separation computed in the spanwise direction ($\mathbf{r}e_2$).

Eulerian statistics can be computed by introducing averages conditioned on a given fluid-flow realization, where the Eulerian RDF is given by

$$\tilde{g}_0(\mathbf{r}e_i) = \frac{\langle \alpha_p(\mathbf{x}, t) \alpha_p(\mathbf{x} + \mathbf{r}e_i, t) \rangle}{\langle \alpha_p(\mathbf{x}, t) \rangle \langle \alpha_p(\mathbf{x} + \mathbf{r}e_i, t) \rangle}, \quad (3.7)$$

and the trace of the Eulerian two-point velocity correlation can be written as

$$\tilde{R}(\mathbf{r}e_i) = \frac{1}{2} \frac{\langle \alpha_p(\mathbf{x}, t) \alpha_p(\mathbf{x} + \mathbf{r}e_i, t) \tilde{\mathbf{u}}_p''(\mathbf{x}, t) \cdot \tilde{\mathbf{u}}_p''(\mathbf{x} + \mathbf{r}e_i, t) \rangle}{\langle \alpha_p(\mathbf{x}, t) \alpha_p(\mathbf{x} + \mathbf{r}e_i, t) \rangle}. \quad (3.8)$$

A key result found in the work by Février *et al.* (2005) is that the mesoscopic Eulerian contribution to the particle-phase velocity accounts completely for the two-point Lagrangian spatial correlations, such that $g_0(\mathbf{r}e_i) = \tilde{g}_0(\mathbf{r}e_i)$ and $R(\mathbf{r}e_i) = \tilde{R}(\mathbf{r}e_i)$. Figure 3 shows comparisons between the two-point Lagrangian correlations (3.5) and (3.6) and two-point Eulerian statistics (3.7) and (3.8) computed using the adaptive filter in the streamwise ($\mathbf{r}e_1$) and spanwise ($\mathbf{r}e_2$) directions. In the limit of pair separation $r \rightarrow 0$, the two-point velocity correlations remain smaller than κ_p , indicating a finite granular temperature. Overall, the adaptive volume filter yields excellent predictions of the spatial correlation of particle position and velocity, providing confidence that the instantaneous spatial distribution is accurately captured from Lagrangian data. Note that the spanwise velocity correlations in figure 3(b) do not approach zero at maximum pair separations, suggesting that the domain size might not be large enough. It remains to be known whether or not the cluster size distribution scales with the size of the domain, and thus we present the largest simulation that remains computationally feasible.

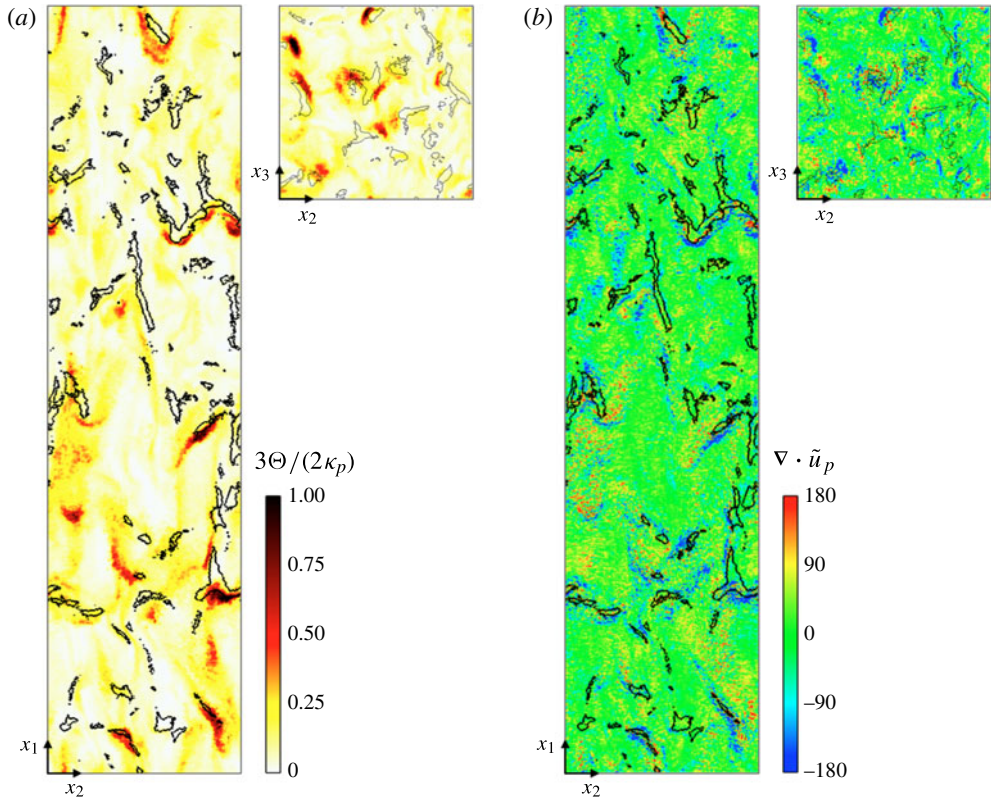


FIGURE 4. Two-dimensional planes from a single realization of fully developed CIT. (a) Granular temperature and (b) divergence of the filtered particle-phase velocity. The black lines show isocontours of $\alpha_p = 3\langle\alpha_p\rangle$. A supplementary movie is available at <http://dx.doi.org/10.1017/jfm.2014.194>.

3.4. Instantaneous results

The adaptive volume filter is applied to an instantaneous field from the simulation using the parameters employed in figure 3. As shown in figure 4, negligible granular temperature is observed within clusters, while maximum values exist just upstream of clusters, where the filtered particle velocity field is locally compressive, i.e. $\nabla \cdot \tilde{\mathbf{u}}_p < 0$. This behaviour is analogous to a highly compressible gas, where the dilatation of the fluid velocity results in compressive heating (Wilcox 2006; Rumsey 2009). Here, compressive heating will yield local regions of high granular pressure, resulting in increased drag and a reduction in cluster fall velocity. As opposed to the reduction in fluid drag seen in clusters due to entrainment of the surrounding fluid, the change in cluster fall velocity due to enhanced granular pressure should arise even in the absence of a carrier phase. Similar behaviour was first observed by Goldhirsch & Zanetti (1993) in the context of a gas–solid homogeneous cooling system. They showed that viscous heating is the dominant effect leading to the development of volume fraction inhomogeneities in dissipative granular flows in the absence of any external forcing (i.e. gravity). In a recent derivation of the Reynolds-average two-equation model for fluid–particle flows, Fox (2014) showed that viscous heating

acts as a source term in the transport of PA granular temperature. This is consistent with the results shown in figure 4.

4. Conclusions and future outlook

In this work, we present results that are part of a long-term study in which we analyse the turbulence characteristics in fully coupled gravity-driven particle-laden flows. We introduce a canonical flow that isolates the effects of momentum coupling between the two phases on the production of fluid-phase turbulence, which we refer to as CIT. The flow is solved in an Eulerian–Lagrangian framework with special care taken during interphase exchange processes to decouple the particle diameter to mesh size ratio. Starting from a random distribution of particles subject to gravity, after an initial transient the flow becomes statistically stationary or fully developed CIT, with a p.d.f. of particle volume fraction that closely resembles a log–normal distribution. The normalized slip velocity $|\mathbf{u}_f - \mathbf{u}_p|/(\tau_p g)$ is observed to be significantly greater than unity in dense regions of the flow, indicating that clusters have lower drag than individual particles. An adaptive spatial filter is employed to separate the instantaneous particle-phase turbulent kinetic energy and granular temperature, and represent them as Eulerian fields. Excellent agreement with two-point Lagrangian statistics is observed, verifying the capability of the filter to accurately extract local instantaneous data. The instantaneous volume-filtered data suggest that granular temperature appears at the upstream boundary of clusters where the particle velocity field is highly compressible, analogously to shock waves in compressible gas flow. Because the fluid-phase turbulence is generated by momentum coupling with the particles, its properties cannot be predicted *a priori*. It remains to be seen how the local and Reynolds-averaged statistics depend on the key dimensionless parameters, the importance of interparticle collisions in determining the turbulence characteristics, and the mechanisms that determine the cluster size distribution.

Acknowledgements

The research reported in this paper is partially supported by the HPC equipment purchased through NSF MRI grant number CNS 1229081 and NSF CRI grant number 1205413.

Supplementary movie

A supplementary movie is available at <http://dx.doi.org/10.1017/jfm.2014.194>.

References

- AGRAWAL, K., LOEZOS, P. N., SYAMLAL, M. & SUNDARESAN, S. 2001 The role of meso-scale structures in rapid gas–solid flows. *J. Fluid Mech.* **445** (1), 151–185.
- ANDERSON, T. B. & JACKSON, R. 1967 Fluid mechanical description of fluidized beds. Equations of motion. *Ind. Engng Chem. Fundam.* **6** (4), 527–539.
- BALACHANDAR, S. & EATON, J. K. 2010 Turbulent dispersed multiphase flow. *Annu. Rev. Fluid Mech.* **42**, 111–133.
- BRILEY, W. R. & McDONALD, H. 1977 Solution of the multidimensional compressible Navier–Stokes equations by a generalized implicit method. *J. Comput. Phys.* **24** (4), 372–397.
- CAPECELATRO, J. & DESJARDINS, O. 2013 An Euler–Lagrange strategy for simulating particle-laden flows. *J. Comput. Phys.* **238**, 1–31.

- CAPECELATRO, J., PEPIOT, P. & DESJARDINS, O. 2014 Numerical characterization and modeling of particle clustering in wall-bounded vertical risers. *Chem. Engng J.* **245**, 295–310.
- CUNDALL, P. A. & STRACK, O. D. L. 1979 A discrete numerical model for granular assemblies. *Géotechnique* **29** (1), 47–65.
- DASGUPTA, S., JACKSON, R. & SUNDARESAN, S. 1994 Turbulent gas–particle flow in vertical risers. *AIChE J.* **40** (2), 215–228.
- EATON, J. K. & FESSLER, J. R. 1994 Preferential concentration of particles by turbulence. *Intl J. Multiphase Flow* **20**, 169–209.
- FÉVRIER, P., SIMONIN, O. & SQUIRES, K. D. 2005 Partitioning of particle velocities in gas–solid turbulent flows into a continuous field and a spatially uncorrelated random distribution: theoretical formalism and numerical study. *J. Fluid Mech.* **533**, 1–46.
- FOX, R. O. 2012 Large-eddy-simulation tools for multiphase flows. *Annu. Rev. Fluid Mech.* **44**, 47–76.
- FOX, R. O. 2014 On multiphase turbulence models for collisional fluid–particle flows. *J. Fluid Mech.* **742**, 368–424.
- GLASSER, B. J., SUNDARESAN, S. & KEVREKIDIS, I. G. 1998 From bubbles to clusters in fluidized beds. *Phys. Rev. Lett.* **81**, 1849.
- GOLDHIRSCH, I. & ZANETTI, G. 1993 Clustering instability in dissipative gases. *Phys. Rev. Lett.* **70** (11), 1619.
- HOPKINS, M. A. & LOUGE, M. Y. 1991 Inelastic microstructure in rapid granular flows of smooth disks. *Phys. Fluids* **3** (1), 47–57.
- HRENYA, C. M. & SINCLAIR, J. L. 1997 Effects of particle-phase turbulence in gas–solid flows. *AIChE J.* **43** (4), 853–869.
- IGCI, Y., ANDREWS, A. T., SUNDARESAN, S., PANNALA, S. & O’BIEN, T. 2008 Filtered two-fluid models for fluidized gas–particle suspensions. *AIChE J.* **54** (6), 1431–1448.
- MAXEY, M. R. 1987 The gravitational settling of aerosol particles in homogeneous turbulence and random flow fields. *J. Fluid Mech.* **174**, 441–465.
- MCQUARRIE, D. A. 1976 *Statistical Mechanics*. Harper and Row.
- MITRANO, P. P., DAHL, S. R., HILGER, A. M., EWASKO, C. J. & HRENYA, C. M. 2013 Dual role of friction in granular flows: attenuation versus enhancement of instabilities. *J. Fluid Mech.* **729**, 484–495.
- OZEL, A., FEDE, P. & SIMONIN, O. 2013 Development of filtered Euler–Euler two-phase model for circulating fluidised bed: high resolution simulation, formulation and a priori analyses. *Intl J. Multiphase Flow* **55**, 43–63.
- POZORSKI, J. & APTE, S. V. 2009 Filtered particle tracking in isotropic turbulence and stochastic modeling of subgrid-scale dispersion. *Intl J. Multiphase Flow* **35** (2), 118–128.
- ROYER, J. R., EVANS, D. J., OYARTE, L., GUO, Q., KAPIT, E., MÖBIUS, M. E., WAITUKAITIS, S. R. & JAEGER, H. M. 2009 High-speed tracking of rupture and clustering in freely falling granular streams. *Nature* **459** (7250), 1110–1113.
- RUMSEY, C. L. 2009 Compressibility considerations for $\kappa - \omega$ turbulence models in hypersonic boundary layer applications. *Tech Rep.* NASA/TM-2009-215705. NASA Center for AeroSpace Information.
- SHAFFER, F., GOPALAN, B., BREault, R. W., COCCO, R., KARRI, S. B., HAYS, R. & KNOWLTON, T. 2013 High speed imaging of particle flow fields in CFB risers. *Powder Technol.* **242**, 86–99.
- SQUIRES, K. D. & EATON, J. K. 1991 Preferential concentration of particles by turbulence. *Phys. Fluids A* **3**, 1169.
- TENNETI, S., GARG, R. & SUBRAMANIAM, S. 2011 Drag law for monodisperse gas–solid systems using particle-resolved direct numerical simulation of flow past fixed assemblies of spheres. *Intl J. Multiphase Flow* **37** (9), 1072–1092.
- TENNETI, S. & SUBRAMANIAM, S. 2014 Particle-resolved direct numerical simulation for gas–solid flow model development. *Annu. Rev. Fluid Mech.* **46**, 199–230.

Particle dynamics in cluster-induced turbulence

- TSUJI, Y., TANAKA, T. & YONEMURA, S. 1994 Particle induced turbulence. *Appl. Mech. Rev.* **47** (6), S75–S79.
- WILCOX, D. C. 2006 *Turbulence Modeling for CFD*. 3rd edn. DCW Industries.
- WYLIE, J. J. & KOCH, D. L. 2000 Particle clustering due to hydrodynamic interactions. *Phys. Fluids* **12** (5), 964–970.
- YIN, X., ZENK, J. R., MITRANO, P. P. & HRENYA, C. M. 2013 Impact of collisional versus viscous dissipation on flow instabilities in gas–solid systems. *J. Fluid Mech.* **727**, R2.